Shielding Properties of Lead-Free Tellurite Glasses against Photons, Neutrons, and Ions

Devendra Raj Upadhyay[1,3], **Suffian Mohamad Tajudin**[2] **and Raju Khanal**[1]

[1]Central Department of Physics, Tribhuvan University, Kirtipur, Kathmandu, Nepal
[2]School of Medical Imaging, Sultan Zainal Abidin University, Terengganu, Malaysia
[3]Department of Physics, Amrit Campus, Tribhuvan University, Thamel, Kathmandu, Nepal
devendra.upadhyay@ac.tu.edu.np

1 Abstract

The shielding capabilities of five different glass systems, namely $60TeO_2$–(30-x)ZnO–$5Bi_2O_3$–$5TiO_2$-xB_2O_3, where x varies from 0 to 10 mol%, against photons, protons, alpha particles, neutrons, and carbon ions were investigated. The study involved the theoretical analysis and Monte Carlo simulations of various shielding parameters such as attenuation coefficients, mean free path, value layers, effective atomic number, effective electron density, and build-up factors, spanning an energy range from 1 keV to 100 GeV. Additionally, rapid neutron removal cross-sections and effective conductivity for the transport properties of the glass compositions were examined. The simulation utilized the glass samples as shielding materials and subjected them to bombardment by photons emitted from Cs^{137} and Co^{60} sources. Stopping potentials and projected range of protons, alpha particles, and ions were also analyzed using the Stopping and Range of Ions in Matter (SRIM) software. The results indicated that the glass composition $60TeO_2$–30.0ZnO–$5Bi_2O_3$–$5.0TiO_2$ exhibited superior attenuation capabilities against gamma rays in comparison to other samples. Conversely, the glass composition $60TeO_2$–20.0ZnO–$5Bi_2O_3$–$5TiO_2$-$10.0B_2O_3$ displayed excellent protons, alpha particles, carbon ions and neutron shielding behavior owing to its higher boron atom concentration. By comparing the calculated attenuation parameters, potentials, and ranges with previously reported data and recommended glass systems for nuclear applications, it is concluded that the selected glass sample demonstrated effective and comparable shielding properties. This study provides valuable insights into the shielding properties of different glass compositions against diverse radiation types. These findings are crucial for the development of shielding materials for nuclear applications and environments with potential radiation exposure.

2 Materials and Methods

Table 1: Chemical composition of glass samples and density [1].

S.N.	Composition (mole %)	x	g cm^{-3}
S_1	$60TeO_2$–30.0ZnO–$5Bi_2O_3$–$5TiO_2$	0.0	5.879
S_2	$60TeO_2$–27.5ZnO–$5Bi_2O_3$–$5TiO_2$ – $2.5B_2O_3$	2.5	5.819
S_3	$60TeO_2$–25.0ZnO–$5Bi_2O_3$–$5TiO_2$ – $5.0B_2O_3$	5.0	5.780
S_4	$60TeO_2$–22.5ZnO–$5Bi_2O_3$–$5TiO_2$ – $7.5B_2O_3$	7.5	5.665
S_5	$60TeO_2$–20.0ZnO–$5Bi_2O_3$–$5TiO_2$ – $10.0B_2O_3$	10.0	5.646

Work Flow [1-5]

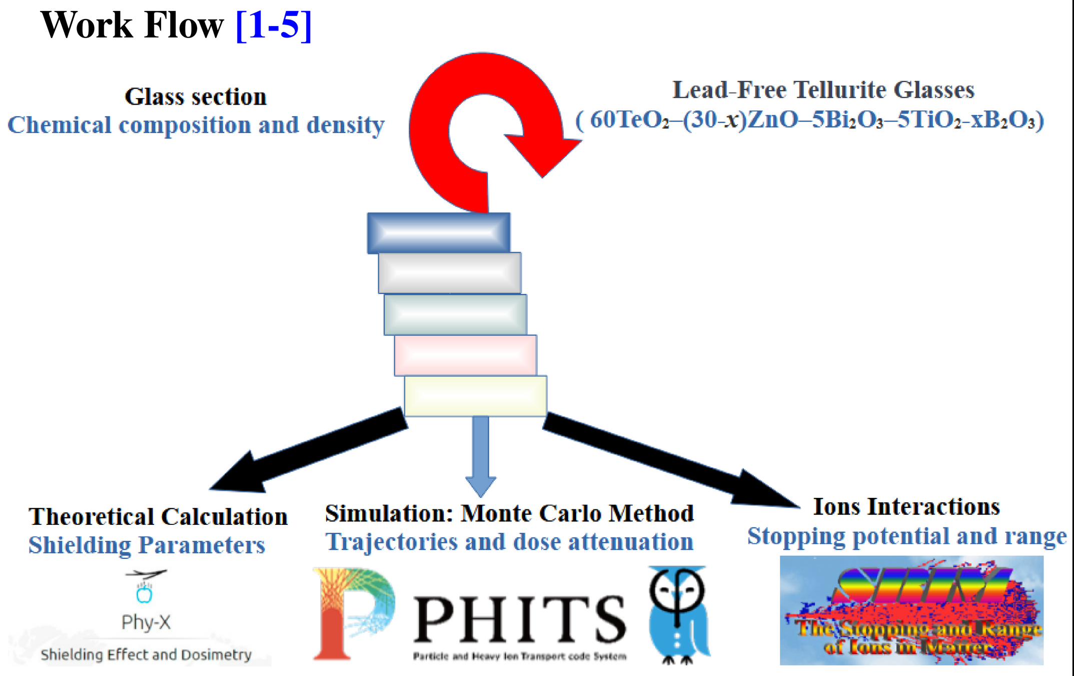

Theoretical Framework [2-5]

$$\mu_m = \frac{\mu}{\rho} \quad (1)$$

$$HVL = \frac{0.692}{\mu} \quad (2)$$

$$TVL = \frac{2.302}{\mu} \quad (3)$$

$$MFP = \frac{1}{\mu_m \rho} \quad (4)$$

$$Z_{eff} = \frac{\sigma_a}{\sigma_e} \quad (5)$$

$$N_{eff} = \frac{\mu_m}{\sigma_e} \quad (6)$$

$$C_{eff} = \left(\frac{N_{eff}\rho\tau e^2}{m_e}\right)10^3 \quad (7)$$

$$\frac{dE}{dx} = K\left(\frac{Z}{A}\right)\frac{z^2}{\beta^2}\rho\left(\ln\left(\frac{2m_e v^2\gamma^2 T_{max}}{I^2}\right) - \beta^2\right) \quad (8)$$

where, μ, μ_m = Mass, linear attenuation coefficient, ρ= density of materials, HVL, TVL= half, tenth value layer, MFP = mean free path, Z_{eff} = effective atomic number, σ_a, σ_e= atomic and electronic cross sections, N_{eff}, C_{eff} = effective electron density, conductivity, m_e, e = mass and charge of electron, τ = relaxation time, $\frac{dE}{dx}$ = stopping potential, v = velocity of particles, A = Atomic mass, K = a constant factor = 0.1535 MeV cm^2 g^{-1}, z = Charge of the particle, γ = Lorentz factor = $\frac{1}{\sqrt{(1-\beta^2)}}$, T_{max}= maximum energy transfer in a single collision, I = mean excitation energy of the material

3 Results and Discussion

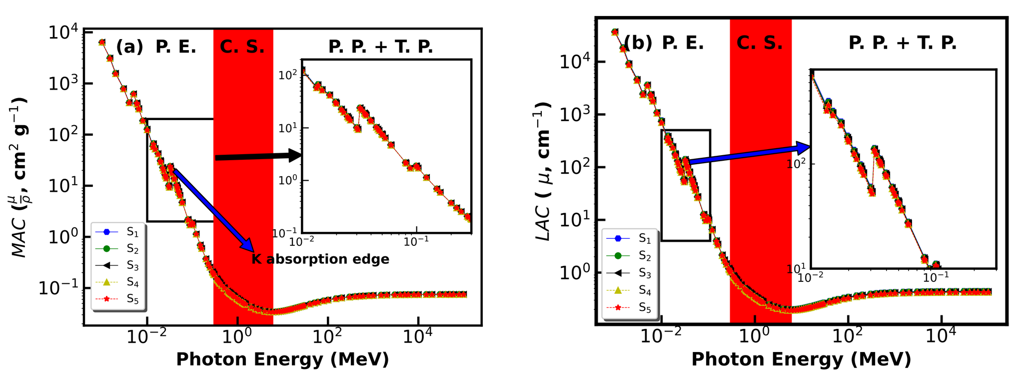

Fig. 1. Alteration in attenuation coefficients for the selected glass systems: $60TeO_2$–(30-x)ZnO–$5Bi_2O_3$–$5TiO_2$-xB_2O_3 as the function of incident energy of the photon (a) mass attenuation coefficient. (b) linear attenuation coefficient from Phy-X/PSD.

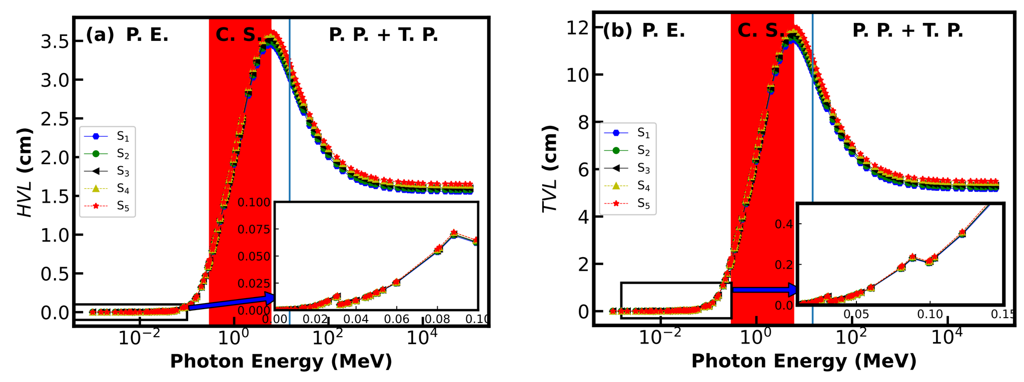

Fig. 2. Variation of value layer for glass systems as the function of incident energy (a) Half (b) Tenth.

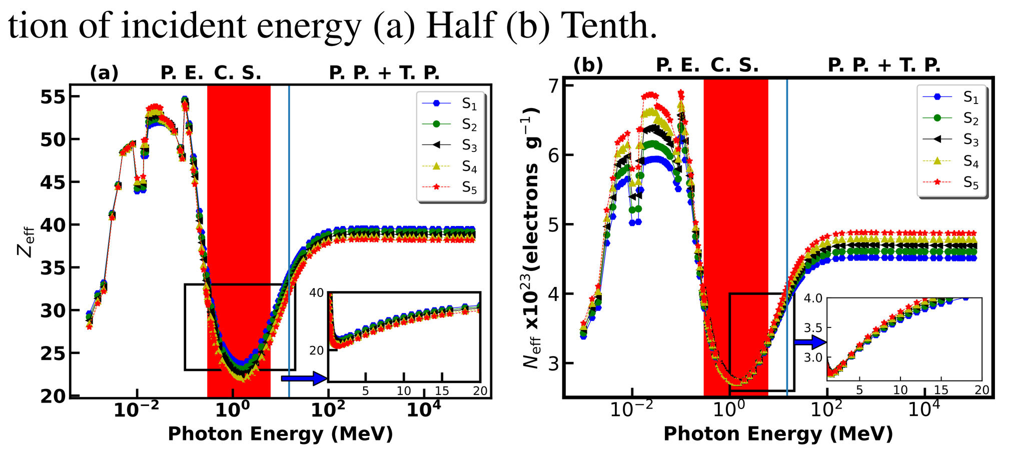

Fig. 3. (a) effective atomic number (b) effective electron density.

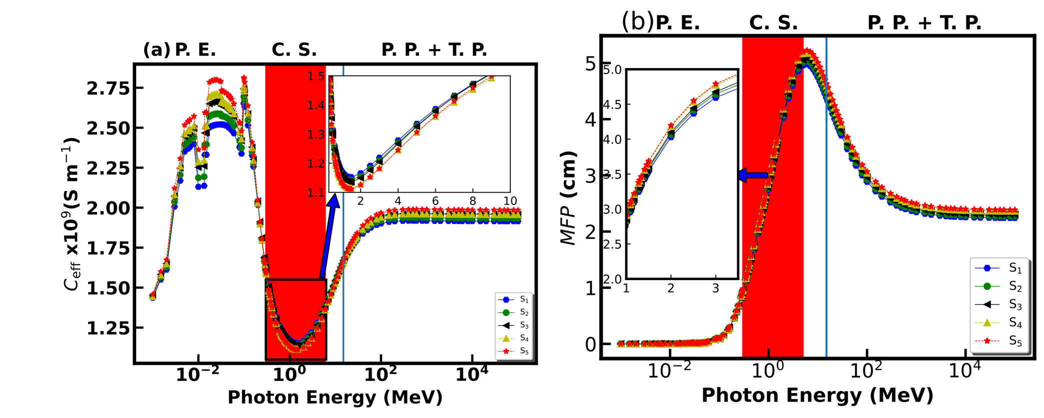

Fig. 4. (a) Effective conductivity and (b) mean free path.

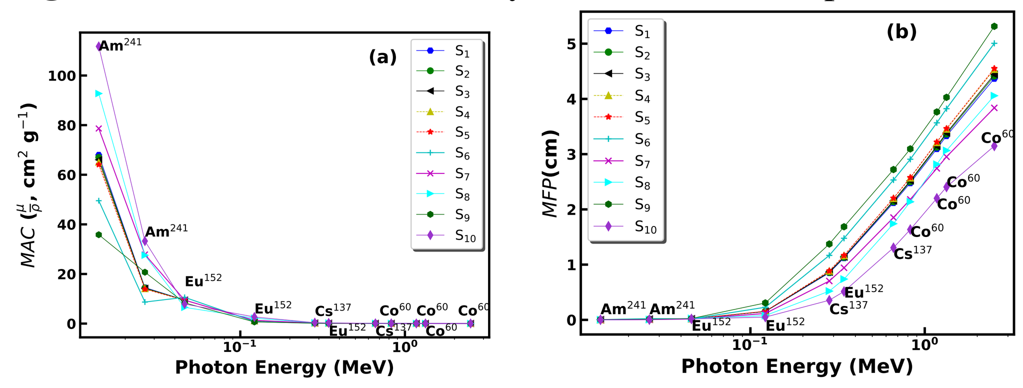

Fig. 5. Variation of (a) MAC values and (b)MFP for glass system: $60TeO_2$–(30-x)ZnO–$5Bi_2O_3$–$5TiO_2$-xB_2O_3 at several gamma energy from Eu^{152}, Am^{241}, Cs^{137} and Co^{60}.

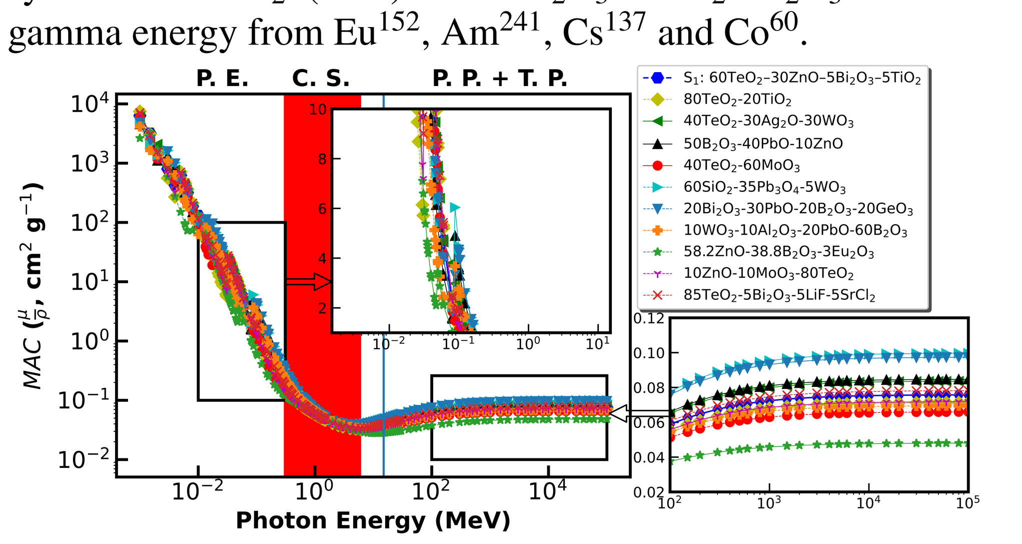

Fig. 6. Comparison of MAC values of S_1 glass system with previous published work.

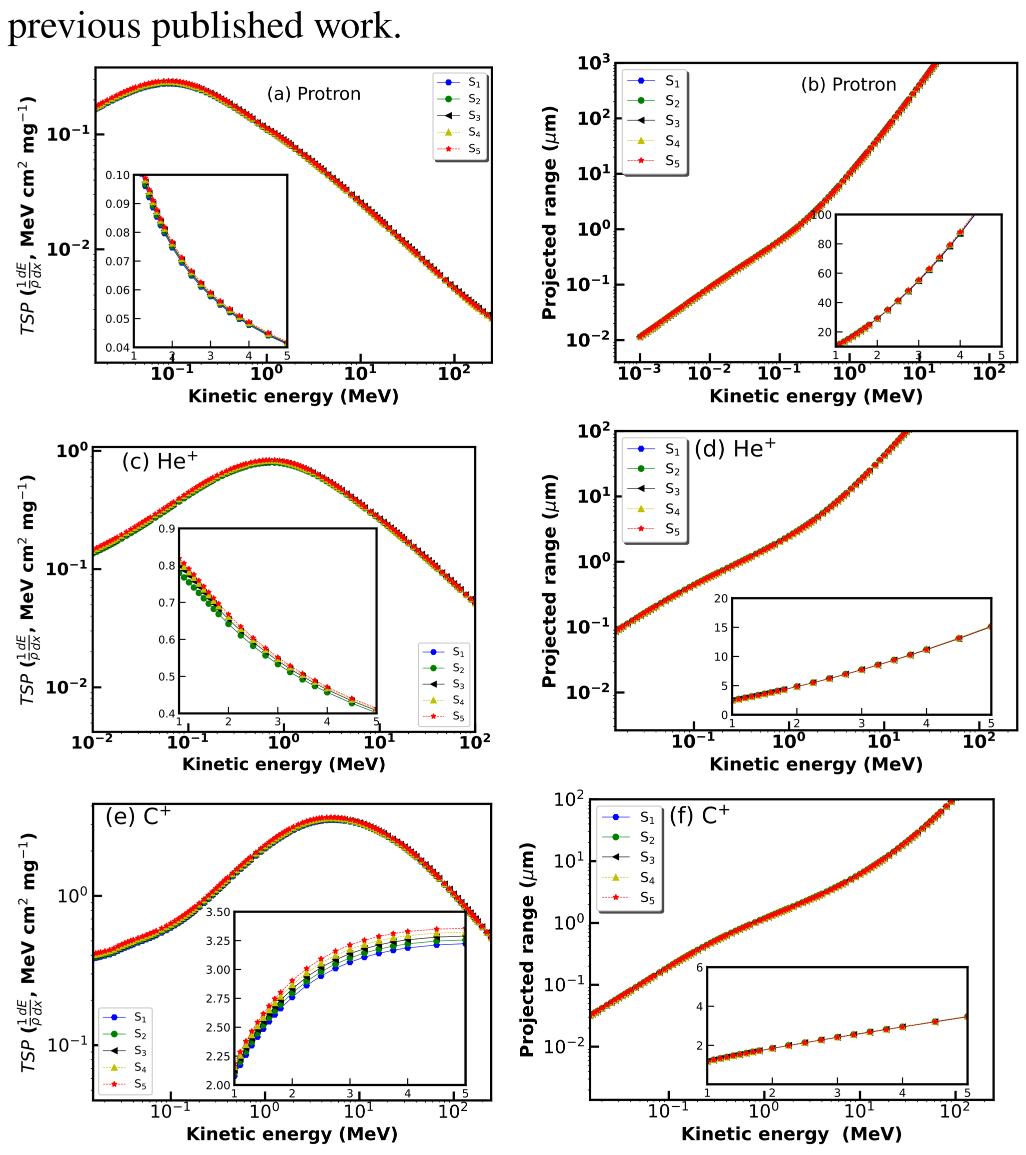

Fig. 7. (a) H^+ total stopping potential (TSP), (b) H^+ projected range (PR) (c) He^+ TSP (d) He^+ PR, and (e) C^+ TSP and (f) C^+ PR by $60TeO_2$–(30-x)ZnO–$5Bi_2O_3$–$5TiO_2$-xB_2O_3 glass system.

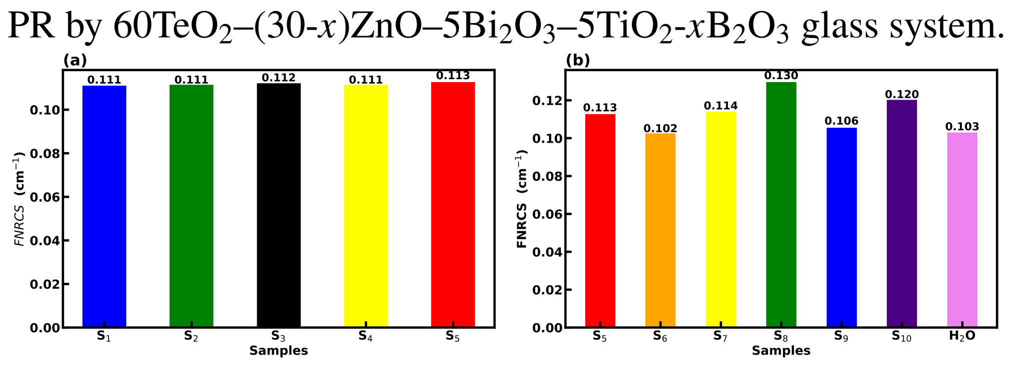

Fig. 8. Fast neutron removal cross section (a) selected samples and (b) S_5 and previously recommended glass samples for nuclear application samples.

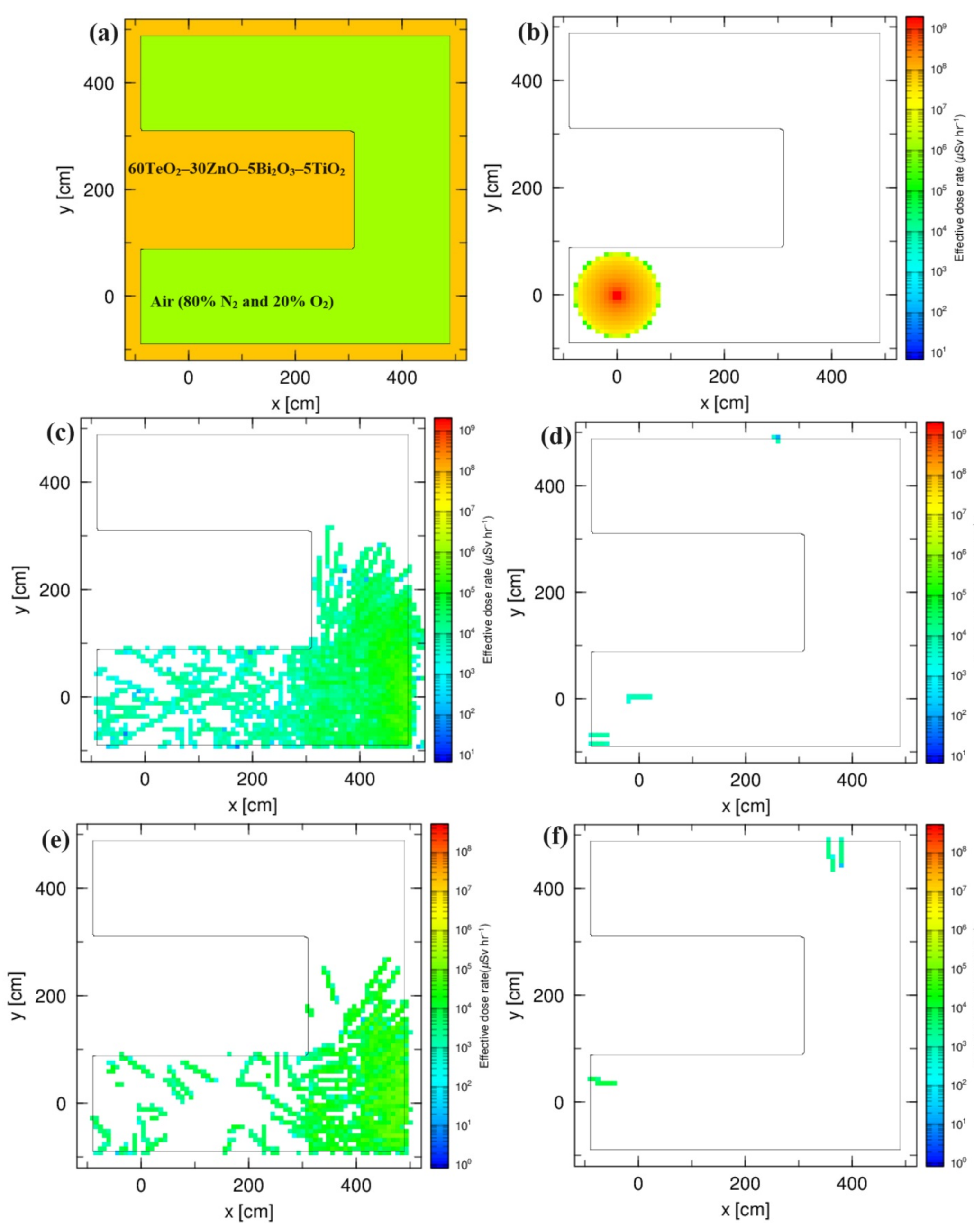

Fig. 9. (a) Geometry consist of Air (80% N_2 and 20% O_2) and S_1 glass system. (b) bombarded 10^5 photon at instant from artificial radionuclei, Co^{60} of 200 GBq source after 2.5 nsec. (c) Co^{60} (200 GBq) 10^5 photon trajectories inside the system at time 20 nsec (d) Cs^{137} (200 GBq) gamma photon trajectories inside the system at time 37.5 nsec, (e) Cs^{137} (200 GBq) 10^5 photon trajectories inside the system at time 20 nsec, (f) Cs^{137} (200 GBq) 10^5 photon trajectories inside the system at time 37.5 nsec.

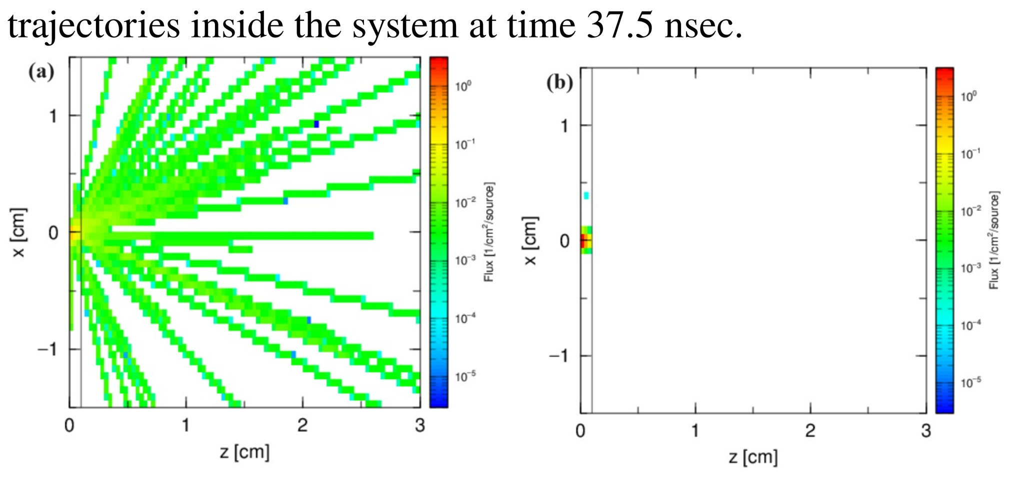

Fig. 10. (a) Photon (b) electron shielding by 0.1 cm glass with energy range up to 1 GeV.

4 Conclusions

- The attenuation of photons is greater for S_1 ($60TeO_2$–30.0ZnO–$5Bi_2O_3$–$5.0TiO_2$), whereas transport properties, ion stopping potentials, and the fast neutron removal parameter are higher for S_5 ($60TeO_2$–20.0ZnO–$5Bi_2O_3$–$5TiO_2$-$10.0B_2O_3$), suggesting that for photons, density matters. However, for charged particles and neutron protective capability, it depends upon the chemical composition of materials. Here, boron concentrations play a role in better shielding against neutrons and ions.
- Using the PHITS Monte Carlo method and SRIM, the selected glass demonstrates comparable attenuating properties to those previously reported for accelerator and nuclear applications.
- Present studied glasses have potential applications as shielding materials against photons, neutrons, and ions, serving as a lead-free alternative.

5 Acknowledgements

- Office of Radiological Security, U.S. Department of Energy: for support to participate in the AccelApp'24
- Jefferson Lab, ANS, IAEA, Pacific Northwest National Laboratory: for invitation and support
- IAEA (TC Project NEP0002): for nuclear lab facilities
- University Grants Commission, Nepal: for Ph.D. fellowship (Ph.D. 78/79-S&T-14)

References

[1] Marzuki et al. (2022). Effect of B_2O_3 addition on thermal and optical properties of TeO_2-ZnO-Bi_2O_3-TiO_2 glasses. Materials Research Express, **9**(2), 025203.

[2] Şakar et al. (2020). Phy-X/PSD: development of a user friendly online software for calculation of parameters relevant to radiation shielding and dosimetry. Radiation Physics and Chemistry, **166**, 108496.

[3] Sato et al. (2018). Features of particle and heavy ion transport code system (PHITS) version 3.02. Journal of Nuclear Science and Technology, **55**(6), 684-690.

[4] Ziegler et al. (2010). SRIM–The stopping and range of ions in matter (2010). Nuclear Instruments and Methods in Physics Research Section B: Beam Interactions with Materials and Atoms, **268**(11-12), 1818-1823.

[5] Knoll (2010). Radiation detection and measurement. John Wiley & Sons.